Draft notes, 2008–2015

Non-Specular Scattering in Solar Coronagraphs: A Micro-Rough Guide

Steven R. Cranmer

Department of Astrophysical and Planetary Sciences, Laboratory for Atmospheric and Space Physics, University of Colorado, Boulder, CO 80309, USA

ABSTRACT

This document summarizes a set of calculations that was done to estimate the amount of non-specular scattering in a solar coronagraph, given a primary reflecting mirror with specific aberrations and roughness properties.

1. Introduction

These notes were compiled in 2008 as an informal reference for ongoing design efforts of space-based solar coronagraphs that operate in the ultraviolet (typically 300 to 1300 Å) and may observe the extended solar corona at distances ranging between 0.1 and 10 solar radii ($R_\odot$) from the surface. We are mainly concerned with normal-incidence mirrors for which the main "specular" beam from the bright solar disk has been already occulted or trapped out of the system. We are concerned with understanding the *non-specular scattering* due to the imperfect mirror surface, which can make light from the solar disk masquerade as light from the extended corona.

The ideas discussed below are only one theorist's (probably naïve) interpretation of the problem of non-specular scattering. There is nothing really new here that cannot be found in the references cited below. However, we anticipate that this development may be helpful to other astrophysicists approaching these issues for the first time. A further development of these ideas, with specific application to the UVCS instrument on *SOHO,* was published by Cranmer et al. (2010).

This document is organized as follows. In § 2, we define the statistical and geometrical properties of the system. In § 3, we give a straightforward "semi-empirical" approach to deriving the non-specular scattering from an incident point-source, In § 4 we derive the results of the previous section more rigorously using the Born approximation of scattering theory. In § 5, more attention is paid to the expected angular extent of the (diffraction-dominated) specular beam. Finally, in § 6 we discuss the relative contributions of incident "beams" from various locations on the solar disk, and in § 7 we make some very rough comparisons with real optical systems.

2. Definitions

Let us assume that the mirror in question has an average surface shape that is flat and horizontal, with coordinates x and y spanning the surface area. (We ignore the overall parabolic or spherical shape of a focusing mirror because the micro-roughness to be studied is usually on a scale much smaller than the large-scale curvature.) The random microscopic "bumpiness" of the mirror is described by a height profile $z(x,y)$. We assume the zero-level of this profile is equal to the mean height, or "ideal figure" of the mirror,

$$\langle z \rangle = \frac{\int dx\,dy\; z(x,y)}{\int dx\,dy} = 0\;, \tag{1}$$

where the integrals are taken over the mirror area. The root-mean-square (r.m.s.) surface roughness σ is defined to be the square root of the variance,

$$\langle z^2 \rangle = \frac{\int dx\,dy\; z(x,y)^2}{\int dx\,dy} = \sigma^2\;. \tag{2}$$

Note that the quantity σ conveys no information about the *horizontal* distribution of microscopic structures on the surface. To characterize these, we define the autocorrelation function

$$C(s,t) = \frac{\int dx\,dy\; z(x,y)\,z(x-s,y-t)}{\int dx\,dy} \tag{3}$$

and we assume that there is nothing preferred about either the x or y directions, so that for such an "isotropic surface," $C(s,t) = C(t,s)$ and the autocorrelation function must be a function of a single variable $C(r)$, where $r = (s^2+t^2)^{1/2}$. Note that $C(0) = \sigma^2$, and $C(r)$ decreases below this peak value as r increases.

Initially, we assume that the incident beam of light comes from a point-source on the sky and strikes the mirror at nearly normal incidence. We separate the present problem (of non-specular scattering) from standard geometrical optics by assuming that we *know* exactly the location of the specularly reflected beam, and our goal is to measure the degree of scattering at a relative angular distance θ away from that specular beam. Figure 1 illustrates this geometry, where the specular angles of incidence and reflection are not labeled, but they are assumed to be both: (1) equal in magnitude to one another, and (2) close enough to the surface normal to be able to ignore all obliquity effects (i.e., projection effects of due to the beam intercepting the mirror at an intermediate angle).

The incoming and reflected rays have vector wavenumbers $\mathbf{k}_1$ and $\mathbf{k}_2$, respectively, which have equal magnitudes $k = 2\pi/\lambda$. We also define the scattering vector

$$\mathbf{q} = \mathbf{k}_2 - \mathbf{k}_1 \tag{4}$$

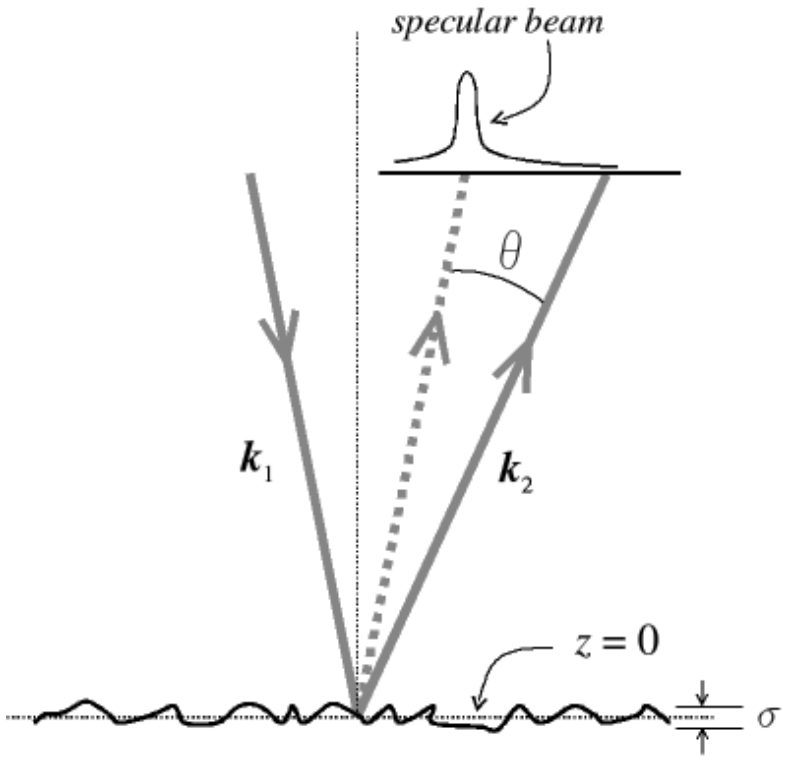

Fig. 1.— *Schematic illustration of normal-incidence scattering geometry.*

where the magnitude $|\mathbf{q}| \approx 2k$. Because of the assumption of normal incidence, we can also assume that $q_z \approx 2k$, and that

$$q_r = (q_x^2 + q_y^2)^{1/2} \approx k \sin\theta \approx 2\pi\theta/\lambda \ll q_z \,. \tag{5}$$

The above approximations assume small angles such that $\sin\theta \approx \theta$. The quantity θ/λ is sometimes called the horizontal "spatial frequency" and is expressed in units of cycles/mm.

3. Simple Semi-Empirical Approach

We begin with a well-known expression for the total integrated scatter (TIS) from a rough surface:

$$\mathrm{TIS} = 1 - e^{-(2k\sigma)^2} \tag{6}$$

where TIS is defined as the ratio of the non-specularly reflected intensity to the total (specular plus non-specular) reflected intensity.[1] This expression was derived originally by Davies (1954) for the scattering of radar waves from the wavy surface of the sea (see also Bennett & Porteus 1961; Bennett 2003). We derive it from more basic principles below in § 4.

In the limit $\sigma \to 0$ (i.e., a perfectly smooth mirror), TIS $\to 0$ as well because all of the intensity will go into the specular beam. The above formula assumes that $\sigma \ll \lambda$, and in this limit, we can write

$$\mathrm{TIS} \approx (2k\sigma)^2 = \frac{16\pi^2\sigma^2}{\lambda^2} \ll 1 \; . \tag{7}$$

The next task is to determine how the non-specular light is *distributed in angle* around the central specular beam. In other words, we wish to determine the point-spread function PSF(θ), for which we define

$$\mathrm{TIS} = \int d\Omega \, \mathrm{PSF}(\theta) = 2\pi \int_{\theta_{\mathrm{min}}}^{\infty} d\theta \, \theta \, \mathrm{PSF}(\theta) \tag{8}$$

where the angular integration of the non-specular beam is taken from some minimum angle θ_{min} (which defines the "size" of the specular beam itself) out to a maximum angle (defined by the macroscopic mirror geometry) that for all practical purposes can be substituted with infinity. For extremely well-polished optics to be flown in space, we can often assume that θ_{min} is given by the diffraction limit,

$$\theta_{\mathrm{min}} = 1.22 \frac{\lambda}{D} \tag{9}$$

where D is the aperture diameter, equivalent to the mirror's physical diameter in most telescopes. We will find below that for "rougher" optics, the effective value of D (which we will call D_{eff}) becomes smaller than the mirror's macroscopic size and is related to the autocorrelation function given above in equation (3).

Let us make an empirically based assumption that the angular dependence of the PSF is a power-law, such that we can define

$$\mathrm{PSF}(\theta) = K\theta^{-\alpha} \tag{10}$$

for the relevant range of angles. We note that $\alpha \approx 3$ is often found experimentally for astronomical mirrors. The integral in equation (8) can thus be performed analytically, to obtain

$$\mathrm{TIS} = \frac{2\pi K}{(\alpha - 2)\,\theta_{\mathrm{min}}^{\alpha-2}} \tag{11}$$

[1] The fraction of specularly reflected intensity (1 − TIS) is related to, but not exactly the same, as the so-called *Strehl ratio,* which is defined as the ratio of the central intensity ($\theta = 0$) for an imperfect mirror to the central intensity for a perfect mirror (with, e.g., $\sigma = 0$).

which applies only for $\alpha > 2$. Thus, if we use the experimentally validated exponent $\alpha = 3$, as well as the approximation for TIS in equation (7), we can solve for K and obtain

$$\mathrm{PSF}(\theta) = \frac{8\pi\sigma^2\theta_{\mathrm{min}}}{\lambda^2\theta^3} \approx 30.66\,\frac{\sigma^2}{\lambda D_{\mathrm{eff}}\theta^3} \ . \tag{12}$$

In the sections below, we will find that this is only one component of the total PSF of the system.

In any case, we wish to determine the so-called *stray light fraction* due to this kind of scattering; i.e., the ratio of scattered specific intensity in a particular (off-limb) location to the intensity of incident light from the solar disk.[2] The PSF has the units of inverse steradians, and is often written as the fraction of incident intensity which is scattered into a differential solid angle:

$$\mathrm{PSF} \equiv \frac{1}{I_0}\frac{dI}{d\Omega} \ .$$

In the optics community, this quantity is sometimes also called the bidirectional reflectance distribution function (BRDF). Thus, the stray light fraction essentially has units of the ratio (dI/I_0), and we must multiply the PSF by the actual solid angle $d\Omega_\odot$ that is subtended by the incident "point source."

To avoid potential confusion about the units (which the author possessed in abundance), we can also derive the stray light fraction in an alternate way. Let us compute the total numbers of photons both coming from the solar disk, and entering an observed resolution element in the extended corona. The total flux (photons s^{-1} cm^{-2}) that is incident from a small "patch" of the solar disk is given by

$$F_\odot = I_\odot\, d\Omega_\odot \ . \tag{13}$$

If the patch is made bigger, more photons enter the system, but the solar-disk intensity $I_\odot$ is assumed not to change. The TIS is essentially defined as the ratio of total scattered photon flux to the total incoming photon flux (the latter being $F_\odot$). Thus, the total non-specular photon flux scattered *into a specific resolution element* a distance θ away from the specular beam is given straightforwardly by

$$F_{\mathrm{scat}} = F_\odot\,\mathrm{PSF}(\theta)\, d\Omega_{\mathrm{element}} \ . \tag{14}$$

Similarly to the above, if the resolution element is made bigger, more scattered photons are measured. However, the *intensity* of photons hitting the resolution element does not depend on the size of the element, and it is given by

$$I_{\mathrm{scat}} = \frac{F_{\mathrm{scat}}}{d\Omega_{\mathrm{element}}} \ . \tag{15}$$

[2]We ignore the fact that no actual mirror is a perfect reflector, and thus we assume that the "solar disk intensity" can be computed from the total reflected intensity by applying the known reflectivity and efficiency factors of the system.

Thus, the stray light ratio is given by

$$\frac{I_{\rm scat}}{I_\odot} \;=\; {\rm PSF}(\theta)\, d\Omega_\odot \;. \tag{16}$$

For an extended object like the Sun, we will eventually sum over a large number of small patches $d\Omega_\odot$ (see § 6), each of which subtends a different scattering angle θ between the solar disk and the desired point above the limb.

4. Alternate Derivation: Born Theory

These derivations mainly follow those of Sinha et al. (1988), Church & Takacs (1993), and Gullikson et al. (1997). We begin with the expression for the differential cross section for scattering of radiation by an arbitrary distribution of matter. The simplest way to express this is by using the so-called *Born approximation,* for which

$$\frac{d\sigma}{d\Omega} = B \int d^3\mathbf{r} \int d^3\mathbf{r}'\; e^{-i\mathbf{q}\cdot(\mathbf{r}-\mathbf{r}')} \;. \tag{17}$$

The differential cross section is closely related to the PSF as defined above.[3] One can see that it is a function of the constant B and the scattering vector $\mathbf{q}$ (see eq. [4]), but there is also a "hidden" dependence on the statistical properties of the mirror surface.

The constant B will eventually not be needed to compute dimensionless ratios such as TIS or the stray light fraction. In X-ray scattering theory, $B = n^2\ell^2$, where n is the number density of scatterers and ℓ is a characteristic scattering length. We find, from a practical standpoint, that one can use

$$B \;=\; \frac{16\pi^2\mathcal{R}}{\lambda^4} \tag{18}$$

where $\mathcal{R}$ is the mirror's overall reflectivity (i.e., reflection coefficient). For example, $\mathcal{R} = 1$ is a "perfect" mirror with infinite conductivity, and other values $\mathcal{R} < 1$ can be computed by using the standard Fresnel equations and the refractive index of the mirror-surface material.

Equation (17) has the general form of a Fourier transform, and the similarity to Fraunhofer diffraction theory will become apparent below. We can use the Divergence Theorem to transform the volume integrals above into surface integrals (taking the mean plane $z = 0$ as the surface over which to integrate), and

$$\frac{d\sigma}{d\Omega} = \frac{B}{q_z^2} \int dx\, dy \int dx'\, dy'\; e^{-i\mathbf{q}\cdot(\mathbf{r}-\mathbf{r}')} \;. \tag{19}$$

[3]We note that the symbol σ in the numerator of $d\sigma/d\Omega$ is completely unrelated to the r.m.s. surface roughness σ used elsewhere.

The exponential in the integrand can be expanded out in more detail as

$$e^{-i\mathbf{q}\cdot(\mathbf{r}-\mathbf{r}')} = \exp\{-iq_x(x-x')-iq_y(y-y')-iq_z[z(x,y)-z(x',y')]\} \ . \tag{20}$$

The two integrals over the mirror surface ($dx\,dy$ and $dx'\,dy'$) cover the same limits as in the statistical definitions from § 2. We can rearrange the variables in a more straightforward way by defining relative coordinates $s = x-x'$, $t = y-y'$, and rewrite the integrals as

$$\frac{d\sigma}{d\Omega} = \frac{B}{q_z^2}\int ds\,dt\,e^{-i(q_x s+q_y t)}\int dx\,dy\,\exp\{-iq_z[z(x,y)-z(x-s,y-t)]\} \ . \tag{21}$$

The right-most integration in equation (21) is immediately recognizable as being of the same form as equations (1)–(3). Thus, our immediate goal is to understand the statistics of the so-called height-height correlation variable $u \equiv z(x,y)-z(x-s,y-t)$, and we wish to know how to express the moment $\langle e^{-iq_z u}\rangle$ in terms of the known statistical properties of our mirror.

We immediately note that equation (1) can be used to show that

$$\langle u\rangle = 0 \ , \tag{22}$$

and we can use equations (2) and (3) to show that

$$\langle u^2\rangle = 2\sigma^2 - 2C(s,t) \equiv g(s,t) \tag{23}$$

where $g(s,t)$ is sometimes called the *structure function.* Next, we must make a critical assumption that the underlying statistics follow a normal, or Gaussian distribution in the variable u. In other words, the moments can be defined in an alternate way as

$$\langle f(u)\rangle = \int_{-\infty}^{+\infty} du\,p(u)\,f(u) \tag{24}$$

where the normalized probability distribution for u is assumed to be

$$p(u) = \frac{1}{\sqrt{2\pi g}}\,e^{-u^2/(2g)} \ . \tag{25}$$

Rakels (1996) discussed how some of the basic properties of specular reflection change when one assumes departures from Gaussian statistics, but for the rest of this document we will keep this assumption.

In order to compute the moment $\langle e^{-iq_z u}\rangle$, we can expand the argument as a power series,

$$e^{-iq_z u} = 1 - iq_z u - \frac{q_z^2 u^2}{2!} + \frac{iq_z^3 u^3}{3!} + \frac{q_z^4 u^4}{4!} - \cdots \tag{26}$$

and thus the moment averaging can be done term-by-term. Because $p(u)$ is symmetric around zero, all of the odd moments vanish, and we are left with

$$\langle e^{-iq_z u}\rangle = \sum_{n=0}^{\infty} \frac{(-1)^n q_z^{2n}\langle u^{2n}\rangle}{(2n)!} \,. \tag{27}$$

Using the Gaussian probability distribution (eq. [25]), we find that

$$\langle u^{2n}\rangle = \frac{g^n\,(2n)!}{2^n\,n!} \tag{28}$$

and thus

$$\langle e^{-iq_z u}\rangle = \sum_{n=0}^{\infty} \left(\frac{-q_z^2 g(s,t)}{2}\right)^n \frac{1}{n!} = e^{-q_z^2 g(s,t)/2} \,. \tag{29}$$

Thus, we can write the differential cross section as

$$\frac{d\sigma}{d\Omega} = \frac{BA}{q_z^2}\int ds\,dt\,\exp\left[-\frac{q_z^2 g(s,t)}{2} - i(q_x s + q_y t)\right] \tag{30}$$

where A is the total mirror area (given as the normalizing factor $\int dx\,dy$ in eqs. [1]–[3]). The above is equivalent to equation (2.11) of Sinha et al. (1988), the derivation of which was unfortunately not described in as much detail as above.

We can also simplify the above expression by taking account of the assumed "isotropic" nature of the mirror; i.e., by expressing everything in terms of $r = (s^2+t^2)^{1/2}$ and $q_r = (q_x^2+q_y^2)^{1/2}$. We can also define the angles

$$\phi = \tan^{-1}(t/s)\,, \quad \psi = \tan^{-1}(q_y/q_x) \tag{31}$$

and express

$$\exp(-iq_x s - iq_y t) = \exp[-iq_r r(\cos\phi\cos\psi + \sin\phi\sin\psi)] = \exp[-iq_r r\cos(\phi-\psi)] \,. \tag{32}$$

We can also make use of the identity

$$2\pi J_0(z) = \int_0^{2\pi} e^{iz\cos\phi'}\,d\phi' \tag{33}$$

to convert the integral in equation (30) from Cartesian to polar coordinates:

$$\frac{d\sigma}{d\Omega} = \frac{2\pi BA}{q_z^2}\int_0^{\infty} dr\,r\,\exp\left[-\frac{q_z^2 g(r)}{2}\right] J_0(q_r r) \,. \tag{34}$$

Note that the limits of the r integration have been extended to infinity because the macroscopic size of the mirror is assumed to be much larger than the sizes of the surface-roughness features that are

being considered here. (See § 5 for more about the implications of ignoring the finite size of the mirror.)

Computing the angular distribution of scattering has been reduced to an integral over a function of the roughness σ and autocorrelation C of the mirror (recall that the structure function $g = 2\sigma^2 - 2C$). We can make use of a commonly used (and empirically derived) parameterization for the autocorrelation function,

$$C(r) = \sigma^2 \exp\left[-\left(\frac{r}{\xi}\right)^{2h}\right] \tag{35}$$

where ξ is the horizontal *correlation length* (or coherence length) of the mirror and h is a texture parameter that describes how smooth or jagged the surface features are. Small values ($h \ll 1$) indicate extremely jagged surfaces and large values ($h \to 1$) describe smooth crests and troughs. No matter the value of h, though, when $r = \xi$ the autocorrelation has dropped to $1/e$ of its central value.

Let us use the above form for the autocorrelation function and rewrite equation (34) as

$$\frac{d\sigma}{d\Omega} = \frac{2\pi BA}{q_z^2} e^{-q_z^2\sigma^2} \int_0^\infty dr\, r\, J_0(q_r r)\, \exp\left[q_z^2\sigma^2 e^{-(r/\xi)^{2h}}\right] . \tag{36}$$

We recall from § 3 that the overall surface roughness σ is small compared to the wavelength λ, so the right-most exponential will have a value very close to 1. We will thus separate it into two pieces that we will find can be called "specular" and "scattered:"

$$\exp\left[q_z^2\sigma^2 e^{-(r/\xi)^{2h}}\right] = f_{\rm spec} + f_{\rm scat} \tag{37}$$

where

$$f_{\rm spec} = 1 \tag{38}$$

$$f_{\rm scat} = \exp\left[q_z^2\sigma^2 e^{-(r/\xi)^{2h}}\right] - 1 \approx q_z^2\sigma^2 e^{-(r/\xi)^{2h}} \ll 1 . \tag{39}$$

Note something interesting that has happened for the scattered part of the cross section. Inserting $f_{\rm scat}$ into equation (36) above essentially gives the Fourier transform of the autocorrelation function. The Wiener-Khinchin theorem tells us that the Fourier transform of an autocorrelation function is indeed the *power spectrum* of the fluctuations. This is directly related to the distribution of intensity scattered away from the specular beam.

As we evaluate the integrals for the specular and scattered parts of the beam, we can also simplify by noting that the differential cross section $d\sigma/d\Omega$ is closely related to the definition of the PSF as given earlier. Specifically,

$$\frac{1}{I_0}\frac{dI}{d\Omega} = \frac{1}{A}\frac{d\sigma}{d\Omega} \tag{40}$$

(e.g., Gullikson et al. 1997), and it is also common to define the *power spectral density* (PSD) as

$$\text{PSD} \equiv S(\mathbf{q}) = \frac{1}{B}\left(\frac{1}{I_0}\frac{dI}{d\Omega}\right) \tag{41}$$

which we will use below.

Using the above definitions, the specular integral can be performed by making use of the orthogonality of Bessel functions, to find

$$S_{\text{spec}}(\mathbf{q}) = \frac{2\pi}{q_z^2} e^{-q_z^2\sigma^2}\,\frac{\delta(q_r)}{q_r}\,. \tag{42}$$

From this delta-function form, we can understand why this piece of equation (37) was identified with the specular beam.

In general, the scattered (non-specular) integral can be written as

$$S_{\text{scat}}(\mathbf{q}) = 2\pi\sigma^2\xi^2 e^{-q_z^2\sigma^2} N_h(q_r\xi)\,, \tag{43}$$

where the dimensionless function $N_h(a)$ is defined as

$$N_h(a) = \int_0^\infty dx\, x\, J_0(ax)\, e^{-x^{2h}}\,. \tag{44}$$

There are only two discrete values of h for which this integral can be evaluated analytically: $h = 1/2$ and $h = 1$. Using various Bessel-function identities, one obtains

$$N_{1/2}(a) = \frac{1}{(1+a^2)^{3/2}}\,, \quad N_1(a) = \frac{1}{2}e^{-a^2/4} \tag{45}$$

and thus

$$S_{\text{scat}}(\mathbf{q}) = \pi\sigma^2\xi^2 e^{-q_z^2\sigma^2} \begin{cases} 2(1+q_r^2\xi^2)^{-3/2}\,, & h = 1/2 \\ \exp\left(-q_r^2\xi^2/4\right)\,, & h = 1\,. \end{cases} \tag{46}$$

Figure 2 shows the result of integrating equation (44) numerically for a range of h values between 0.3 and 0.99. For the large values of a that we will find useful below, we find that N_h behaves more or less as a power law, with the exponent ranging from about −2.7 (for $h = 0.3$) to −4.5 (for $h = 0.9$).

Elson et al. (1993) gave a parameterization for the autocorrelation function that is a linear superposition of the $h = 1/2$ ("long-range") and $h = 1$ ("short-range") analytic terms. The special value $h = 1/2$ is also often identified as a "conventional surface finish," and we will restrict ourselves to this for the remainder of this section.[4]

[4]Sinha et al. (1988) and Church & Takacs (1993) go into much more detail about other values of h and other possible forms for the autocorrelation function (including fractals).

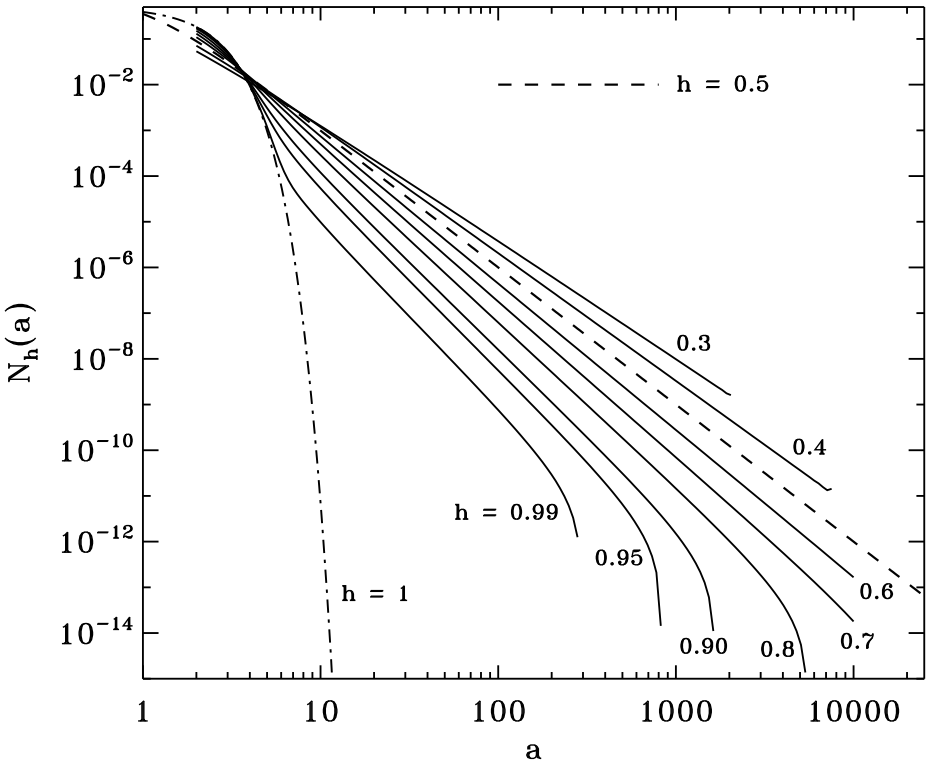

Fig. 2.— *Dimensionless scattering function $N_h(a)$ shown for a range of texture parameters h (see labels for values).*

We can evaluate various quantities to compare with the results from § 3. The TIS can be defined as

$$\mathrm{TIS} = \frac{\int d\Omega\, S_{\mathrm{scat}}}{\int d\Omega\, (S_{\mathrm{scat}} + S_{\mathrm{spec}})} \tag{47}$$

where we note that the solid-angle integral can be written as

$$d\Omega = 2\pi\theta\, d\theta = \frac{\lambda^2}{2\pi} q_r\, dq_r\ . \tag{48}$$

These integrals are straightforward, and

$$\int d\Omega\, S_{\mathrm{spec}} = \frac{\lambda^4}{16\pi^2}\, e^{-q_z^2\sigma^2}\ , \tag{49}$$

$$\int d\Omega\, S_{\mathrm{scat}} = \sigma^2\lambda^2\, e^{-q_z^2\sigma^2}\ , \tag{50}$$

and thus

$$\mathrm{TIS} = \frac{16\pi^2\sigma^2/\lambda^2}{1+(16\pi^2\sigma^2/\lambda^2)} \approx \frac{16\pi^2\sigma^2}{\lambda^2} \tag{51}$$

where the latter is the same as the approximation given in equation (7) for $\sigma \ll \lambda$.

An alternate way to estimate the TIS is to simply compare the PSD for the specular part of the beam to its value for a "flawless" mirror ($\sigma = 0$) for which the specular beam would presumably contain 100% of the reflected intensity. Using equation (42), we find that this ratio is simply given by $e^{-q_z^2\sigma^2}$, and thus the fraction of the intensity going into the non-specular beam (i.e., the TIS) is $1-e^{-q_z^2\sigma^2}$. The latter is exactly what was given in the initial definition of TIS in equation (6).

Next we can simplify the expression for the non-specular scattering function to compare it with the semi-empirical PSF(θ) derived above. Using equation (8) to relate the PSF to TIS, we find that compatibility with equation (50) above demands $B = 16\pi^2/\lambda^4$, or "perfect reflectivity." Thus, we obtain (specifically for the $h = 1/2$ case),

$$\mathrm{PSF} = \frac{1}{I_0}\frac{dI}{d\Omega} = \frac{32\pi^3\sigma^2\xi^2}{\lambda^4(1+q_r^2\xi^2)^{3/2}} \,. \tag{52}$$

In the limit of large correlation lengths ($q_r\xi \gg 1$), this simplifies to

$$\frac{1}{I_0}\frac{dI}{d\Omega} \approx \frac{4\sigma^2}{\lambda\,\xi\,\theta^3} \tag{53}$$

which has the same scalings with wavelength λ, scattering angle θ, and roughness σ as equation (12). If the the correlation length ξ can be considered equivalent to (or at least linearly related to) the effective aperture diameter D_{eff}, then the above differs from equation (12) only by a numerical factor of $1.22(2\pi) \approx 7.7$. In fact, if the definition of the autocorrelation function in equation (35) would have been written instead as

$$C(r) = \sigma^2 \exp\left[-\left(\tilde{k}r\right)^{2h}\right] \,, \tag{54}$$

with $\tilde{k}$ being a *correlation wavenumber,* the corresponding "correlation wavelength" would be defined as $\Lambda = 2\pi/\tilde{k}$. In this case, $\Lambda = 2\pi\xi$, and this would only differ from D_{eff} by a factor of 1.22. In practice, we will utilize the slightly larger numerical factor from equation (12) in our calculations below, which will tend to overestimate the scatter by 22%. If the non-specular scatter is smaller than predicted, then that is a bonus!

5. The Specular Beam: Diffraction Theory with Aberrations

We are concerned with the broadening of the specular beam for optics that are not "diffraction-limited." In other words, we wish to compute the properties of the specular beam for a mirror having large-scale monochromatic aberrations. The magnitude of such aberrations is often described by a single length-scale, called the *r.m.s. wavefront error* ω, which (like the r.m.s. surface roughness

σ) describes the "amplitude" of the mirror-surface distortions. We will first derive the properties of Fraunhofer diffraction for an ideal "perfect" mirror (§ 5.1) then examine how aberrations broaden the specular beam (§ 5.2).

5.1. Diffraction and the Ideal Mirror

Let us begin with an ideal flat mirror, but take more consistent account of its finite size. Although these derivations parallel those in standard texts on astronomical optics (e.g., Born & Wolf 1999; Schroeder 2000), we begin from the Born theory results in the previous section. If we ignore the *statistical* fluctuations of the mirror surface, the mirror height $z(x,y)$ is identically zero everywhere. Thus, equation (19) can be separated into the product of two identical integrals, as

$$\frac{d\sigma}{d\Omega} = \frac{B}{q_z^2}\left|\int dx\,dy\,e^{-i(q_x x+q_y y)}\right|^2 \tag{55}$$

without the need to transform into the relative coordinates s and t. Assuming a circular shape for the mirror, with diameter D, we can transform into polar coordinates as in equation (32), to obtain

$$\frac{d\sigma}{d\Omega} = \frac{B}{q_z^2}\left|\int_0^{D/2} dr\,r\int_0^{2\pi} d\phi\,e^{-iq_r r\cos(\phi-\psi)}\right|^2 = \frac{4\pi^2 B}{q_z^2}\left|\int_0^{D/2} dr\,r\,J_0(q_r r)\right|^2 \tag{56}$$

where, here, $r=(x^2+y^2)^{1/2}$ and $\phi=\tan^{-1}(y/x)$. The azimuthal angle ψ is defined as in equation (31), and we can set it to any arbitrary value (such as zero). This is the standard Fraunhofer diffraction integral for a circular aperture, and it is straightforwardly evaluated to be

$$\frac{d\sigma}{d\Omega} = \frac{BA^2}{q_z^2}\left[\frac{2J_1(v)}{v}\right]^2 \tag{57}$$

where $A=\pi D^2/4$ and we define the variable v to be linearly proportional to q_r (or θ), with

$$v = \frac{q_r D}{2} = \frac{\pi D\theta}{\lambda}\,. \tag{58}$$

The classical "Airy disk" is defined as the first minimum in the above Bessel function quantity, which occurs at $v=1.22\pi=3.832$ (i.e., eq. [9]).

Schroeder (2000) also gives an expression for the averaged PSF in the so-called *Airy wings.* For large arguments ($v \gg 1$), a smoothed version of the Bessel function quantity above is given approximately by

$$\left\langle\left[\frac{2J_1(v)}{v}\right]^2\right\rangle \approx \frac{4}{\pi v^3} \tag{59}$$

and in this limit, we obtain

$$\langle S_{\rm Airy}(\mathbf{q})\rangle = \frac{1}{BA}\frac{d\sigma}{d\Omega} = \frac{D^2}{q_z^2 v^3} \ . \tag{60}$$

We can also use the perfect-mirror expression for $B = 16\pi^2/\lambda^4$ to compute

$$\mathrm{PSF}_{\rm Airy}(\theta) = B\langle S_{\rm Airy}(\mathbf{q})\rangle = \frac{\lambda}{\pi^3 D\theta^3} \tag{61}$$

which can be compared directly to the micro-roughness component of the PSF (eq. [12]),

$$\mathrm{PSF}_{\sigma}(\theta) = 30.66\frac{\sigma^2}{\lambda D_{\rm eff}\theta^3} \ . \tag{62}$$

The actual scattering PSF is a combination of these two effects, and as a worst-case scenario we will add them linearly to one another. Note that they both drop off as θ^{-3}, which means that the relative degree of "competition" between the two effects will remain the same as a function of scattering angle.

5.2. Diffraction and the Aberrated Mirror

For Fraunhofer diffraction off a mirror containing *aberrations,* we must insert a phase factor to the exponent in equation (56) which takes account of the optical path difference between the aberrated wavefronts and the ideal, non-aberrated wavefronts. We define the wavefront path difference as $\Phi(r,\phi)$, and we write a more general version of the differential cross section:

$$\frac{d\sigma}{d\Omega} = \frac{BA}{\pi q_z^2}\left|\int_0^1 d\rho\,\rho\int_0^{2\pi} d\phi\,\exp[i(k\Phi - v\rho\cos(\phi-\psi)]\right|^2 \tag{63}$$

where we adopt the dimensionless radial distance $\rho = 2r/D$. The above agrees with equation (56) when $\Phi = 0$. Note that, in general, the above integral contains real and complex parts which must be computed separately.

We use the definitions of orthogonal third-order aberrations in terms of Zernike polynomials as given in, e.g., Table 10.6 of Schroeder (2000). For a circular aperture without any central obstruction, we can define various types of aberrations and compute the r.m.s. wavefront errors associated with each:

Spherical	$\Phi = a_{40}\left(\rho^4 - \rho^2 + \frac{1}{6}\right)$	$\omega/\lambda = \lvert a_{40}\rvert/(6\sqrt{5})$
Coma	$\Phi = a_{31}\left(\rho^3 - \frac{2}{3}\right)\sin\phi$	$\omega/\lambda = \lvert a_{31}\rvert/(6\sqrt{2})$
Astigmatism	$\Phi = a_{22}\rho^2\left(\sin^2\phi - \frac{1}{2}\right)$	$\omega/\lambda = \lvert a_{22}\rvert/(2\sqrt{6})$
Defocus	$\Phi = a_{20}\left(\rho^2 - \frac{1}{2}\right)$	$\omega/\lambda = \lvert a_{20}\rvert/(2\sqrt{3})$
Distortion	$\Phi = a_{11}\rho\sin\phi$	$\omega/\lambda = \lvert a_{11}\rvert/2$

(64)

which assumes in each case that *all* of the wavefront error is attributed to only one type of aberration.

For known values of ω and v, equation (63) can be evaluated numerically for each type of aberration. Let us also adopt more standard terminology from the astronomical optics texts. For example, Schroeder (2000) defines the dimensionless complex wave amplitude as

$$U(v,\psi) = \int_0^{2\pi} d\phi \int_0^1 d\rho\, \rho\, \exp\left[i(k\Phi - v\rho\cos(\phi-\psi)\right] \tag{65}$$

with the dimensionless intensity (proportional to eq. [63]) given by

$$i(v) = |U(v)|^2 \,. \tag{66}$$

The so-called *encircled energy* inside a given radius v_0 is defined as

$$\mathrm{EE}(v_0) = \int_0^{v_0} dv\, v\, i(v) \tag{67}$$

where the above quantities are given to within an arbitrary multiplicative constant. For a non-aberrated mirror, $\omega = 0$, and we showed above that

$$i(v) \propto \left[\frac{2J_1(v)}{v}\right]^2 \,. \tag{68}$$

As $v_0 \to \infty$, EE approaches a constant total energy that encompasses the entire beam. At the radius of the classical Airy disk (i.e., $v = 1.22\pi = 3.832$), the value of EE there is 0.838 times its maximum at $v \to \infty$. This EE criterion is often taken as the standard definition of the specular beam.

For a range of r.m.s. wavefront errors and the five types of aberration defined above, we computed the values of v_0 for which EE was given by 0.838 times its asymptotic value at infinity. We rescaled this resulting angular size into a relative "departure" from the diffraction limit. Aberrations result in broader PSF's than the diffraction limit, but this corresponds to an effective aperture diameter D_{eff} that is *smaller* than the actual diameter D. Thus, Figure 3a plots the ratio

$$\frac{D}{D_{\mathrm{eff}}} = \frac{v_0}{1.22\pi} \geq 1 \tag{69}$$

as a function of the r.m.s. wavefront error in units of wavelengths (i.e., ω/λ).[5] In other words, for $D/D_{\mathrm{eff}} = 2$, the specular beam is twice as broad as the diffraction-limited beam (and is 4 times larger in area), but the value of D_{eff} to use in, e.g., equation (12) is $1/2$ of the actual diameter D.

[5]This latter quantity is typically given as a reciprocal number; i.e., $\omega = \lambda/N$ for a given wavelength, so that $\omega/\lambda = 1/N$.

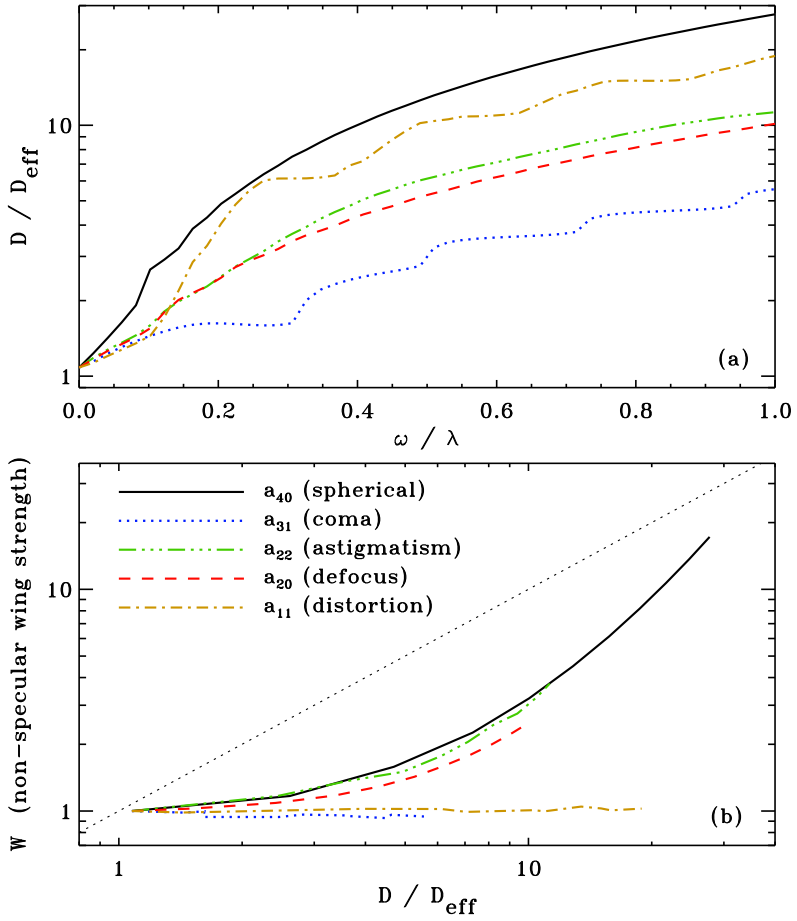

Fig. 3.— *PSF broadening above the diffraction limit due to orthogonal mirror aberrations.* **(a)** *The ratio* $D/D_{\rm eff}$ *is shown as a function of normalized wavefront error* ω/λ *for the assumptions that the aberrations are all of a given type (see labels).* **(b)** *Relative strength* W *of the non-specular "Airy wing" for aberrated beams, shown in units of the ideal non-aberrated wing (eq. [61]).*

There are some correspondences that can be made between the "macro-roughness" of this section and the statistical "micro-roughness" of the previous section. $D_{\rm eff}$ is a reasonably close match to what is meant by the correlation length ξ in § 4, but because the overall spatial scales (macro vs. micro) differ, these two quantities are not exactly the same. Similarly, both the wavefront error ω and the micro-roughness σ are r.m.s. mirror-height amplitudes. In § 4, though, we did not consider the ability of nonzero σ to broaden the specular beam because we derived everything in the limit $\sigma \ll \lambda$. Figure 3a shows that in the similar limit $\omega \ll \lambda$ there would also be no significant effect. Clearly, if $\sigma \sim \lambda$, the derivations of § 4 would have to be redone without the small-σ approximation.

We also note that the "aberrated" intensity pattern $i(v)$ also contains a broadened Airy wing,

analogous to that given in equation (61). We expect that larger aberrations will give rise to a stronger wing. For the numerical models discussed above, we determined the strength of this wing by computing the average of $v^3 i(v)$ for all $v > v_0$ (i.e., only *outside* the broadened specular beam). We define the dimensionless quantity W as the ratio of this average wing strength to the ideal (non-aberrated) value of $4/\pi$ (see eq. [59]). Figure 3b plots W as a function of $D/D_{\rm eff}$ for the five types of aberration discussed above. For some types of aberration (e.g., coma and distortion), the strength of the Airy wing is essentially the same as the non-aberrated value, and $W \approx 1$ even when $D/D_{\rm eff} \gg 1$. For other types (e.g., spherical and astigmatic), the wing is more intense for larger aberrations.

The maximum wing strength shown in Figure 3b corresponds to spherical aberrations, and we fit that dependence of W on $D/D_{\rm eff}$ as a quadratic,

$$W \approx 1 + \frac{D/D_{\rm eff}}{139.4} + \frac{(D/D_{\rm eff})^2}{48.5} \, . \tag{70}$$

However, since the exact form of the aberrations is not known in general, we may sometimes wish to fold in a "safety factor" and assume a slightly larger value of W than given in Figure 3b. Such a safe upper limit can be placed by setting $W \approx D/D_{\rm eff}$ (i.e., the black dotted line). This means that one may just be able to replace D by $D_{\rm eff}$ in equation (61) to obtain a conservative *upper limit* on the scattering in the Airy wing. In this case, the upper limit for the total PSF would be given by the sum

$$\mathrm{PSF}(\theta) = \mathrm{PSF}_{\rm Airy}(\theta) + \mathrm{PSF}_{\sigma}(\theta) \approx \frac{\lambda}{\pi^3 D_{\rm eff} \theta^3} + 30.66 \frac{\sigma^2}{\lambda D_{\rm eff} \theta^3} \tag{71}$$

which can be written as

$$\mathrm{PSF}(\theta) \approx \frac{\lambda}{\pi^3 D_{\rm eff} \theta^3} \left\{ 1 + \left[\frac{\sigma}{\lambda/30.83} \right]^2 \right\} \tag{72}$$

which means that the micro-roughness σ does not seem to be an important contributor to the non-specular scattering unless it is of the order $\sim \lambda/30$ or larger. For the more general case, where W is specified directly on the basis of Figure 3b (or other information), it seems to be more useful to factor out the aberration-independent factor of D, to obtain

$$\mathrm{PSF}(\theta) = \frac{\lambda}{\pi^3 D \theta^3} \left\{ W + \frac{D}{D_{\rm eff}} \left[\frac{\sigma}{\lambda/30.83} \right]^2 \right\} \, . \tag{73}$$

6. Integration over the Solar Disk

The Sun is a distributed source on the sky with a radius given in angular units as $\rho_\odot \equiv 4.65 \times 10^{-3}$ radians = 0.267° = $959.6''$. For the ultraviolet observations with which we are concerned,

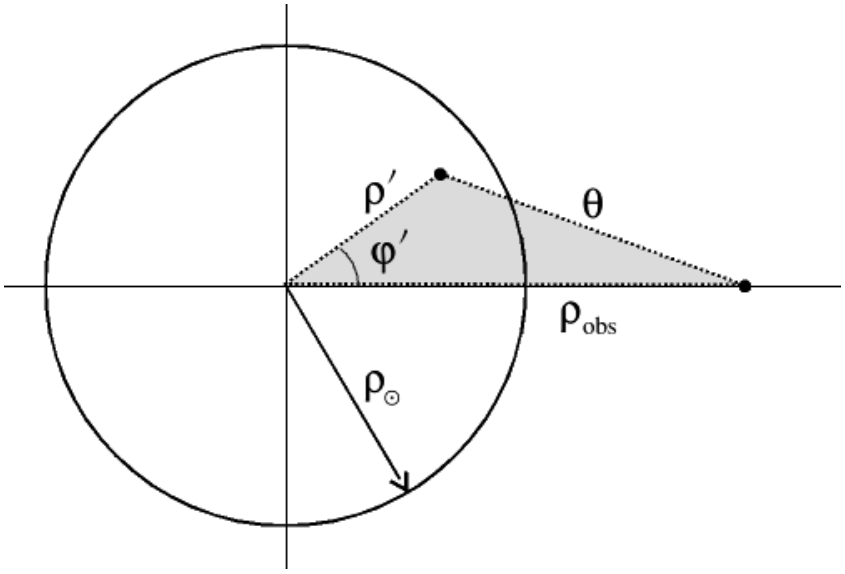

Fig. 4.— *Angular coordinates that define the observed solar disk* (ρ', ϕ')*, the heliocentric observation height* $\rho_{\rm obs}$*, and the angular distance* θ *between each solar-disk specular ray and the non-specular "target."*

there is negligible mean limb-darkening (or limb-brightening) over the solar disk, so we assume the disk is uniformly bright with specific intensity $I_\odot$. Let us define coordinates as in Figure 4, and we integrate equation (16) over the disk as

$$\left(\frac{I_{\rm scat}}{I_\odot}\right)_{\rm total} = \int d\Omega_\odot \, {\rm PSF}(\theta) = \int_0^{2\pi} d\phi' \int_0^{\rho_\odot} d\rho' \, \rho' \, {\rm PSF}(\theta) \tag{74}$$

and

$$\theta^2 = \rho'^2 + \rho_{\rm obs}^2 - 2\rho' \rho_{\rm obs} \cos\phi' \, . \tag{75}$$

The key independent variable is the "observation height" $\rho_{\rm obs}$ which is measured from Sun-center. (For convenience below, we will express $\rho_{\rm obs}$ in solar-radius units, but in the above expressions it must be in the same angular units used for the other quantities.)

There may be an analytic expression for the integral above for the case ${\rm PSF}(\theta) \propto \theta^{-3}$, but it is straightforward enough to integrate it numerically. Figure 5 shows this result, along with three other curves that indicate simpler evaluations that assume *all* of the solar photons come from a point-source on the sky. (These are easier to evaluate using the formulae of §§ 3–5; i.e., using a single value of θ.) Assuming the point-source is at Sun-center underestimates the actual scattering, but begins to approximate the full-disk integration reasonably well above a height of several solar radii. Assuming the point-source is at the nearest limb (directly underneath observation height) always overestimates the actual scattering.

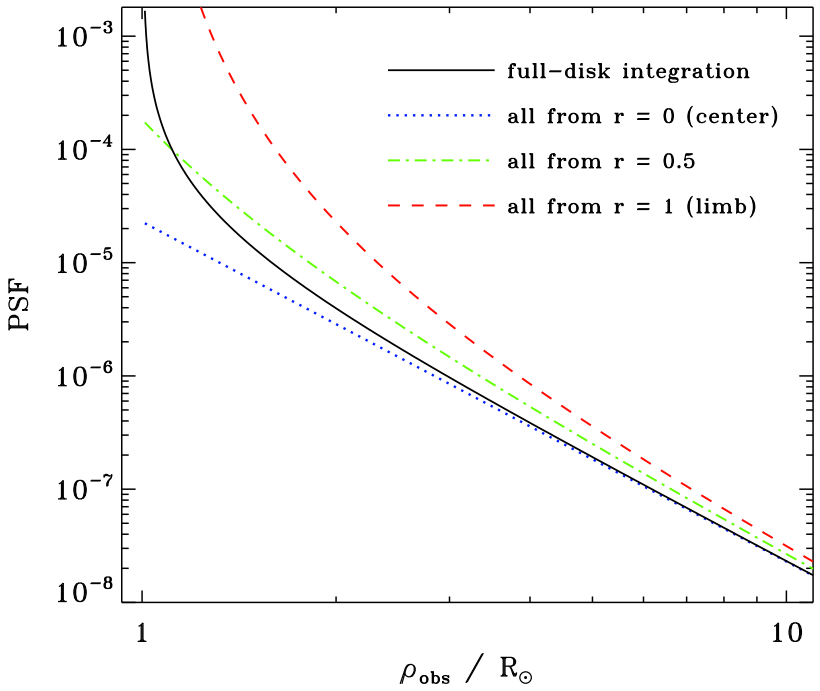

Fig. 5.— PSF(θ) *versus observation height (measured in solar-radius units,* $\rho_{obs}/R_\odot$*) for both a numerical integration over the solar disk (*black solid curve*) and for various assumptions about all solar photons coming from a point-source at disk-center (*blue dotted curve*), from the nearest limb to the the observer (*red dashed curve*), and from a point halfway between the prior two (*green dot-dashed curve*).*

Figure 5 uses equation (72) for the PSF, with assumptions of $\lambda = 1000$ Å, $\sigma = 7.5$ Å (a "modern" achievable value), and a diffraction-limited mirror with $D = D_{\rm eff} = 10$ cm. Note, though, that for these values the Airy wings dominate the non-specular scattering wings by about a factor of 20. (We chose a small value of the micro-roughness, with $\sigma \ll \lambda$, to show that there is likely to be a point of diminishing returns when polishing mirrors down to Ångstrom-level finishes.) Note also that the overall *shape* of the black curve in Figure 5 is valid for any PSF that scales as θ^{-3}.

7. Validation with Real Mirrors

Detailed stray light properties of the *Skylab* SO–55 mirrors were published by Reeves et al. (1977), and we can use them as an example in order to verify the order-of-magnitude accuracy of the above formulae. Figure 8 of Reeves et al. (1977) shows the ratio $I_{\rm scat}/I_\odot$ as a function of height above the limb. For a representative height of 30″ ($\rho_{\rm obs} = 1.031\,R_\odot$), the scattered light ratio is roughly 0.001–0.003.

We can utilize the summed PSF (eq. [72], with safety factor) and perform the numerical integration over the solar disk for this case. The wavelength λ is that of the C III 977 Å line, and the stated r.m.s. micro-roughness σ is 22 Å. The effective aperture $D_{\rm eff}$ that should be used is less certain. The mirror itself has a lateral dimension of $D = 18$ cm, and if it were diffraction-limited it would have an angular resolution of $0.14''$. Reeves et al. (1977), though, gave larger values for the on-sky spatial resolution of $0.4''$ to $1.6''$ (depending on the overall location of the blur pattern in the system). These values were predicted by ray-tracing models that utilized the known off-axis aberrations of the system. This implies that $D_{\rm eff}$ should be *smaller* than the macroscopic mirror dimension. After launch, it was not possible to test this level of resolution because the observations were taken through a $5'' \times 5''$ aperture that acted as the field stop and spectrometer slit. Reeves et al. (1977) stated, though, that the system successfully performed at, or better than, this $5''$ resolution limit.

We can "work backwards" and use the *observed* scattered light ratio of 0.001–0.003, at a height of $30''$ above the limb, to compute the expected angular resolution ($\theta_{\rm min} = 1.22\lambda/D_{\rm eff}$) that would have been needed if our theory for the PSF is valid. Taking a trial value of $\theta_{\rm min} = 1''$, using the equations in §§ 3–5 and the integration over the solar disk in § 6, and the values of λ and σ given above, we find that the following scaling relation applies at a height of $30''$:

$$\left(\frac{I_{\rm scat}}{I_\odot}\right)_{\rm total} = 0.002377 \left(\frac{\theta_{\rm min}}{1''}\right) . \tag{76}$$

In this case, the two terms in equation (72) (i.e., due to the Airy wings and the micro-roughness) are of the same order of magnitude as one another. In order to reproduce the observed scattered light range, the angular resolution $\theta_{\rm min}$ should have been between about $0.42''$ and $1.26''$. These values are very reasonable: they are almost exactly the same as the estimated (ray-traced) range of $0.4''$ to $1.6''$. This can be seen as an order-of-magnitude validation of the non-specular scattering theory derived in this document.

As an independent check, we can also use the r.m.s. wavefront error reported by Reeves et al. (1977) to estimate the departure from the diffraction limit. They gave $\omega = \lambda/10$ for a representative test wavelength of 5461 Å. When applied to the desired UV wavelength of 977 Å, the wavefront error ratio is $\omega/\lambda \approx 0.56$. Examining the range of various types of aberrations from Figure 3a, this translates into a range on $D/D_{\rm eff}$ somewhere between 3.5 and 14.5. The diffraction-limited $\theta_{\rm min}$ of $0.14''$ must then be multiplied by these values, and we obtain a range of $0.5''$ to $2.0''$. This overlaps with the range of 0.42–$1.26''$ derived above using equation (76), and it is also very close to the range of ray-traced spatial resolution values given by Reeves et al. (0.4–$1.6''$). This provides an extra measure of independent verification.

REFERENCES

Bennett, H. E., & Porteus, J. O. 1961, J. Opt. Soc. Am., 51, 123

Bennett, J. M. 2003, "Surface Roughness," in *Encyclopedia of Optical Engineering,* ed. R. G. Driggers, p. 2746 (New York: Marcel Dekker)

Born, M., & Wolf, E. 1999, Principles of Optics: Electromagnetic Theory of Propagation, Interference and Diffraction of Light, 7th ed. (Cambridge, Cambridge U. Press)

Church, E. L., & Takacs, P. Z. 1993, Applied Optics, 32, 3344

Cranmer, S. R., Gardner, L. D., & Kohl, J. L. 2010, "A Model for the Stray Light Contamination of the UVCS Instrument on SOHO," Solar Phys., 263, 275

Davies, H. 1954, Proc. IEE London, 101, 209

Elson, J. M., Bennett, J. M., & Stover, J. C. 1993, Applied Optics, 32, 3362

Gullikson, E. M., Stearns, D. G., Gaines, D. P., & Underwood, J. H. 1997, Proc. SPIE, 3113, 412

Rakels, J. H. 1996, Nanotechnology, 7, 43

Reeves, E. M., Huber, M. C. E., & Timothy, J. G. 1977, Applied Optics, 16, 837

Schroeder, D. J. 2000, Astronomical Optics, 2nd ed. (San Diego: Academic Press)

Sinha, S. K., Sirota, E. B., Garoff, S., & Stanley, H. B. 1988, Phys. Rev. B., 38, 2297